Available online at www.sciencedirect.com

ScienceDirect

Energy Procedia 43 (2013) 27 – 36

Energy Procedia

4th Workshop on Metallization for Crystalline Silicon Solar Cells

The Nature of Screen Printed Front Side Silver Contacts - Results of the project MikroSol

Rene Hoenig[a]*, Michael Duerrschnabel[b], Willem van Mierlo[c], Zainul Aabdin[b], Joerg Bernhard[c], Johannes Biskupek[c], Oliver Eibl[b], Ute Kaiser[c], Juergen Wilde[d], Florian Clement[a], Daniel Biro[a]

[a]*Fraunhofer Institute for Solar Energy Systems ISE, Heidenhofstr. 2, 79110 Freiburg, Germany*
[b]*University of Tuebingen, AG Eibl, Auf der Morgenstelle 10, 72076 Tuebingen, Germany*
[c]*University of Ulm, AG Kaiser, Albert-Einstein-Allee 11, 89081 Ulm, Germany*
[d]*Department of Microsystems Engineering IMTEK, Albert-Ludwigs-University, Georges-Koehler-Allee 103, 79110 Freiburg, Germany*

Abstract

The joint research project *MikroSol* focuses on electrical and microstructural properties of screen printed front side silver contacts. Special attention is given to the contact resistance of the contacts as well as metallization-induced recombination losses in the space charge region of the solar cell. Differently processed industrial solar cells were characterized by electrical measurements as well as analytical electron microscopy including quantitative chemical analyses. The microstructure of these contacts was studied over a large range of length scales from several tens of microns down to a few nanometers. Distinct differences were found for the specific contact resistance depending on the screen printing paste. Microstructural analyses revealed a continuous wetting layer for pastes yielding lower contact resistances. Focused ion beam tomography confirmed the presence of a continuous wetting layer over distances of several microns and revealed new insights about the morphology of front side silver contacts on alkaline textured surfaces. Furthermore, varying densities of nano silver colloids were identified in the continuous glass layer and these colloids were studied by (high-resolution) electron microscopy.

Selection and peer-review under responsibility of Guy Beaucarne, Gunnar Schubert and Jaap Hoornstra

Keywords: front side silver contacts; contact formation; current transport; screen printing; crystalline silicon solar cells

* Corresponding author. Tel.: +49-761-4588-5596
E-mail address: rene.hoenig@ise.fraunhofer.de.

1876-6102
Selection and peer-review under responsibility of Guy Beaucarne, Gunnar Schubert and Jaap Hoornstra
doi:10.1016/j.egypro.2013.11.085

1. Introduction

Understanding the nature of screen printed front side silver contacts is one of the main challenges for metallizing and contacting crystalline silicon solar cells. To further exploit the potential of the industrially attractive screen printing technology, contact formation and current conduction mechanisms need to be identified and evaluated. The quality of the electrical contact between silicon and thick film metallization (specific contact resistance ρ_C) as well as losses due to metallization-induced space charge region recombination (SCR-recombination) are of great relevance. Within *MikroSol* – a joint research project between Fraunhofer ISE and the Universities of Tuebingen and Ulm, financed by the Baden-Wuerttemberg Stiftung gGmbH – extensive investigations of differently processed screen printed front side silver contacts were performed. Therefore, several batches of H-pattern solar cells with aluminum back surface field (Al-BSF) were processed using p-type Czochralski-grown silicon (Cz-Si) wafers. Different material and process parameters were varied, e.g. surface topography, the emitter, the applied screen printing paste, the front side metallization fraction A_{met} and parameters for the rapid thermal firing process (RTF). After processing, macroscopic characterization of the solar cells was performed at Fraunhofer ISE, samples of 10 x 10 mm² area were cut out by a dicing saw and microscopical analyses of the contact structure and the silicon/metallization interface were performed at the universities of Tuebingen and Ulm.

SCR-recombination losses induced by the front side silver contacts of industrial silicon solar cells were mainly macroscopically investigated and results were already published in previous works [1, 2]. In the following, only results regarding contact formation and current transport mechanisms are discussed.

2. Experimental

2.1. Solar cell processing

In several batches, H-pattern Al-BSF solar cells were processed using p-type Cz-Si wafers with a base resistivity ρ_{base} ranging from 1 Ωcm to 6 Ωcm. After alkaline texture in KOH solution, emitter formation was realized by $POCl_3$ diffusion in a tube furnace. Nominal emitter sheet resistances R_{sh} were ranging between 35 Ω/sq and 110 Ω/sq. Most solar cells were processed with an emitter of $R_{sh} \approx 75$ Ω/sq. As passivation and anti-reflection coating (ARC), silicon nitride (SiN_X) layers with a nominal layer thickness of 75 nm to 80 nm were applied by plasma-enhanced chemical vapor deposition (PECVD). Metallization was mainly realized by screen printing, whereas a full-area aluminum layer was printed on the rear side and a H-pattern grid was printed on the front side, using various commercially available front side pastes (FSP) or special test pastes manufactured at Fraunhofer ISE. All pastes were based on silver as the conductive component. The H-pattern grid mainly consisted of two or three busbars and around 50 to 74 contact fingers with a nominal finger width w_f (according to screen printing layout of the computer-aided design) of 50, 90 or 100 µm. Rapid thermal firing (RTF) was carried out either in an industrial conveyor belt furnace (fast firing oven FFO) or in the single wafer reactor *SHS10*. Actual peak wafer temperatures T_{peak} were controlled pyrometrically in the SHS10 or, in most cases, varied by setting the set point peak firing temperature in the fast firing oven T_{FFO}. Apart from empirical knowledge, the offset between actual wafer temperature T_{peak} and T_{FFO} was recorded for firing in the conveyor belt furnace using a K-type thermocouple for selected process groups. Laser edge isolation was always applied for the electrical contact insulation of the wafer edges.

2.2. Macroscopic characterization

For solar cell characterization, current-voltage (*I-V*) measurements (illuminated, dark and Suns-V_{OC} curves) were performed with an industrial solar cell tester under flash illumination based on the spectrum AM1.5G IEC60904-3Ed.2(2008). *I-V* data evaluation always included fill factor loss analyses, as described in [1]. Thereby, most important *I-V* parameters for evaluating process parameters with respect to contact resistance and SCR-recombination were i) series resistance $r_{S,SunsVoc}$ [3] ii) fill factor losses due to series resistance *pFF-FF*, iii) dark saturation current density of the space charge region j_{02} and iv) fill factor losses due to SCR-recombination

FF_0-*pFF* (parallel resistances of the solar cells were in all cases sufficiently high). To visualize series resistance as well as recombination related losses over the whole cell area, the method of a spatially resolved coupled determination of the dark saturation current and series resistance (C-DCR) was applied using photoluminescence (PL) imaging [4]. This method was also used to determine representative regions of the respective solar cells to cut out sample stripes (10 mm in width, length according to cell edge length) for contact resistance measurements applying the transmission line model (TLM) [5]. Within these stripes, several TLM measurements including eight contact fingers were carried out and the most representative cell areas of 10 x 10 mm² (with average values for specific contact resistance ρ_C) were cut out and taken for microstructural analyses of the metal-silicon interface.

Table 1 shows the most important process parameters as well as electrical data of the *I-V* and TLM measurements of four H-pattern Al-BSF Cz-Si solar cells. The solar cells were screen printed with different commercially available screen printing front side silver pastes (*FSP*) and contact fired at two different set point peak firing temperatures T_{FFO} leading to significantly different global series resistances $r_{S,SunsVoc}$ series resistance related fill factor losses *pFF-FF* and therewith conversion efficiencies η. Apparently, $r_{S,SunsVoc}$ as well as *pFF-FF* correlates well with the specific contact resistances ρ_C measured by TLM. *FSP2* and *FSP3* provide significantly lower ρ_C values, although all process parameters were kept constant. Only differences in height and density of the alkaline textured Cz-Si pyramids – which can influence the contact behaviour of the screen printing pastes [6, 7] – are possible, as samples #3 and #4 were processed in different batches as samples #1 and #2. The impact of "overfiring" (too high T_{FFO} applied) on ρ_C is also obvious, when comparing sample #1 and #2 processed with exactly the same process parameters except for the significantly higher T_{FFO} of sample #1. The samples displayed in Table 1 were extensively analysed by means of microscopical characterization and the results are shown in the following.

Table 1 : Process parameters as well as electrical data of *I-V* and TLM measurements for four differently screen printed or fired (alkaline textured) H-pattern Al-BSF Cz-Si solar cells (156 x 156 mm²) processed within MikroSol. Significant differences in specific contact resistance ρ_C and therewith global series resistance $r_{S,SunsVoc}$ and efficiency η of the solar cells due to the applied front side silver paste (FSP) and set point peak firing temperature T_{FFO} in the conveyor belt furnace are clearly visible.

Sample	Paste	Nominal finger width w_f (µm)	T_{FFO} (°C)	η (%)	j_{SC} (mA/cm²)	V_{OC} (mV)	*pFF* (%)	*FF* (%)	$r_{S,SunsVoc}$ (Ωcm²)	ρ_C (mΩcm²)
#1	FSP1	100	960	13.6	35.88	616.2	82.4	61.8	3.91	131
#2	FSP1	100	900	16.9	36.05	609.4	81.8	77.1	0.87	21
#3	FSP2	90	900	18.0	36.70	619.8	82.5	79.1	0.61	5
#4	FSP3	50	900	18.2	36.81	621.2	82.6	79.4	0.59	1

2.3. Microscopic characterization

Scanning electron microscopy (SEM) as well as transmission electron microscopy (TEM) was carried out by the group *Electron Microscopy and Applied Materials Science* (*AG Eibl*) at the Eberhard Karls University of Tuebingen. All samples were prepared by mechanical grinding and polishing. SEM images were acquired using a *JEOL 6500F* equipped with a detector for backscattered electron (BSE) imaging as well as for energy-dispersive x-ray spectroscopy (EDX). TEM images as well as energy-filtered TEM (EFTEM) images were acquired using a *Zeiss EM912Ω*.

Focused ion beam (FIB) investigations were realized by the *Electron Microscopy Group of Material Sciences* (*AG Kaiser*) at the University of Ulm. Thereby, sample preparation as well as tomography imaging (FIB tomography) of the 3-dimensional structure of the front side silver contacts was carried out using a *Zeiss NVision 40*.

3. Results

The overall aim of *MikroSol* is to understand how contact formation works for front side thick film contacts of industrial silicon solar cells and, even more important, how current is transported from the phosphorous-doped silicon emitter into the contact finger. In literature, three main theories for current transport exist, whereas the dominating current path is still under discussion:
i) Current is transported via silver crystallites (imprints in the silicon surface where silver crystallizes during cooling) contacting the emitter which are either in direct contact to the silver bulk of the contact finger or covered by a thin (up to a few nanometers) glass layer [8-10]. In the latter case, electron tunnelling according to the models of direct tunnelling [11] or Fowler-Nordheim tunnelling [12] is conceivable.
ii) Current flow occurs via the (thin) glass layer between the silicon surface and the contact silver bulk, which can be assisted by nano silver colloids contained in the glass layer [13-15].
iii) Current is transported directly from the emitter into the silver bulk of the contact finger [16, 17].
Up to now, no considerable extensions or alternatives can be given to these, partly contradicting, models. Nevertheless, interesting results which reveal new insights about contact formation and current transport mechanisms of screen printed and fired silver contacts are obtained and partly discussed in the following.

3.1. Influence of firing parameters on the contact resistance

The contact formation was studied by applying different material and process parameters that may influence the microstructure and thus electrical performance of screen printed and fired front side silver contacts. Major focus was set on the dependency of contact formation on different parameters of the contact firing process. Most interesting observations on the dependency of the front contact resistance on different (industrially relevant) contact firing parameters in correlation with the contact microstructure were already previously published [18]. It is shown, that lower cooling rates in combination with higher oxygen concentrations in the firing atmosphere support the formation of larger silver crystallites at the pyramid tips of alkaline textured Cz-Si. These larger tip crystallites are assumed to be mainly responsible for significantly lower (specific) contact resistances, as current paths along the pyramid tips are found to be crucial for current transport [6, 7]. A higher density of nano silver colloids in the glass layer due to the lower cooling rate – the glass has more time to solidify and can therefore incorporate a higher amount of silver in the form of nano colloids – could be another explanation.

3.2. Morphology of screen printed and fired front side silver contacts

The morphology of screen printed and fired silver front side contacts with respect to the distribution of chemical phases has been studied by two-dimensional microscopy applying back-scattered electron imaging in a scanning electron microscope (SEM-BSE) as well as by three-dimensional analyses using focused ion beam tomography (FIB tomography). Fig. 1 shows SEM-BSE images of the samples #1, #2 and #3 (see Table 1) screen printed with different pastes and fired at different set point peak temperatures. The front side of the solar cell was mechanically polished and back-scattered electron imaging was performed in plan view. Thus, in comparison to cross-sectional analysis, more silicon-metal interfaces can be observed at once. Table 2 displays most important process parameters, electrical data obtained by I-V and TLM measurements as well as quantitative evaluations of the phase fractions in the metallization observed by SEM-BSE imaging of these samples. When comparing the well contacted sample #3 (screen printed with *FSP2*) to the insufficiently contacted samples #1 and #2 (both screen printed with worse contacting *FSP1*, #1 additionally overfired), it becomes obvious that a continuous wetting layer seems to be important for realizing low specific contact resistances. Furthermore, a glass layer between the silicon surface and the contact silver bulk – even in the micron range – does not necessarily seem to increase the specific contact resistance. For the best contacted sample #3, (by far) the highest amount of glass could be observed.

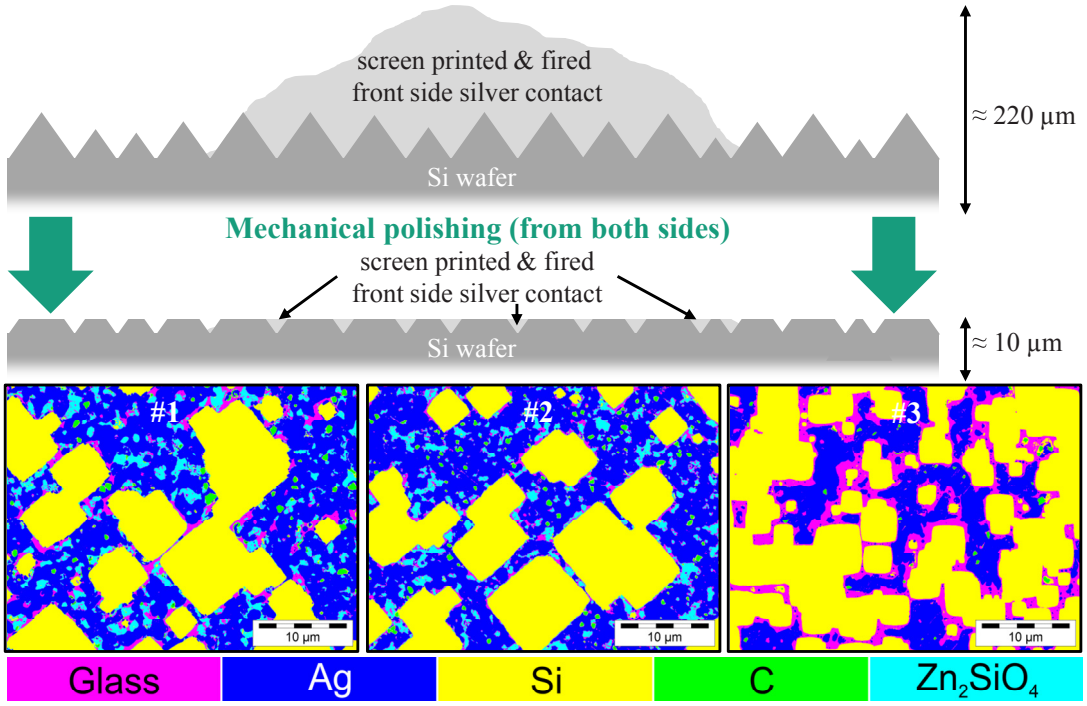

Fig. 1. Phase distribution obtained from BSE images (plan view of mechanically polished front surface) of front side silver contacts screen printed with different pastes and fired at different set point peak firing temperatures after mechanical grinding and polishing of the front surface. All phases observed were identified by spectroscopical analyses using energy-dispersive x-ray spectroscopy in the scanning electron microscope (SEM-EDX). As can be seen, the improved front side paste *FSP2* used for sample #3 shows a better wetting behavior of the glass layer along the silicon surface. Furthermore, no Zn_2SiO_4 phase is observable for this paste. Pores/voids within the metallization are not observable as mechanical polishing can lead to abrasion of the relatively soft silver into the pores.

Table 2: Process parameters, electrical data of TLM measurements as well as quantitative phase fractions of the metallization determined by SEM-BSE imaging for three differently screen printed and fired samples shown in Fig. 1.

Sample	Paste	T_{FFO} (°C)	ρ_C (mΩcm²)	Wetting layer	Ag (%)	Zn_2SiO_4 (%)	Glass (%)
#1	FSP1	960	131	discontinuous	69.6	12.5	16.1
#2	FSP1	900	21	discontinuous	70.7	9.6	18.1
#3	FSP2	900	5	continuous	60.2	-	38.9

This leads to the assumption that current flow through the glass layer plays an important role for the contact performance. Current transport supported by a multi-step tunnelling process along metal precipitates in the glass layer is easily conceivable. Quantitative evaluations of nano silver colloids in the glass layer are displayed in section 3.3. These hypotheses are only valid for the assumption that sufficient electrical contacting appears at this height of the contact (approximately half way between pyramid tips and pyramid valley of the alkaline textured Cz-Si) and current transport along the pyramid tips is not dominating the electrical behavior of the contact, as reported by Cabrera [6, 7]. For more sophisticated and reliable evaluations of the electrical behavior in correlation with the microstructure, the 3D morphology of such contacts has to be taken into account. Therefore, 3D tomography of these samples was performed using a focused ion beam system. Fig. 2 shows a schematic overview of the layer segmentation carried out by FIB tomography for various processed samples with different specific contact resistances (see Table 1). The layers were analyzed with respect to the main chemical phases occurring in the metallization of screen printed and fired front side silver contacts: i) silver, ii) glass, iii) pores.

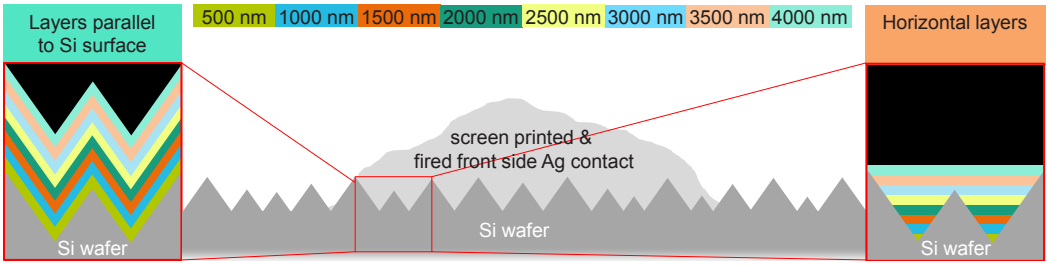

Fig. 2. Schematic of layer segmentation using focused ion beam tomography (FIB tomography). The layers were analyzed according to detectable phases in two ways: i) layers situated parallel to silicon surface, as interesting for current paths between emitter and bulk silver of the contact finger; ii) layers situated horizontal to cross-sectional sample, for height-specific analysis of contact morphology and phase distribution.

Fig. 3 shows the results of FIB tomography layer segmentation carried out for differently processed samples. Samples #1 was screen printed with *FSP1* and overfired (T_{FFO} = 960°C) whereas sample #4 was screen printed with the improved paste *FSP3* and optimally fired (at optimum firing temperature of T_{FFO} = 900°C) showing a significantly lower specific contact resistance after firing.

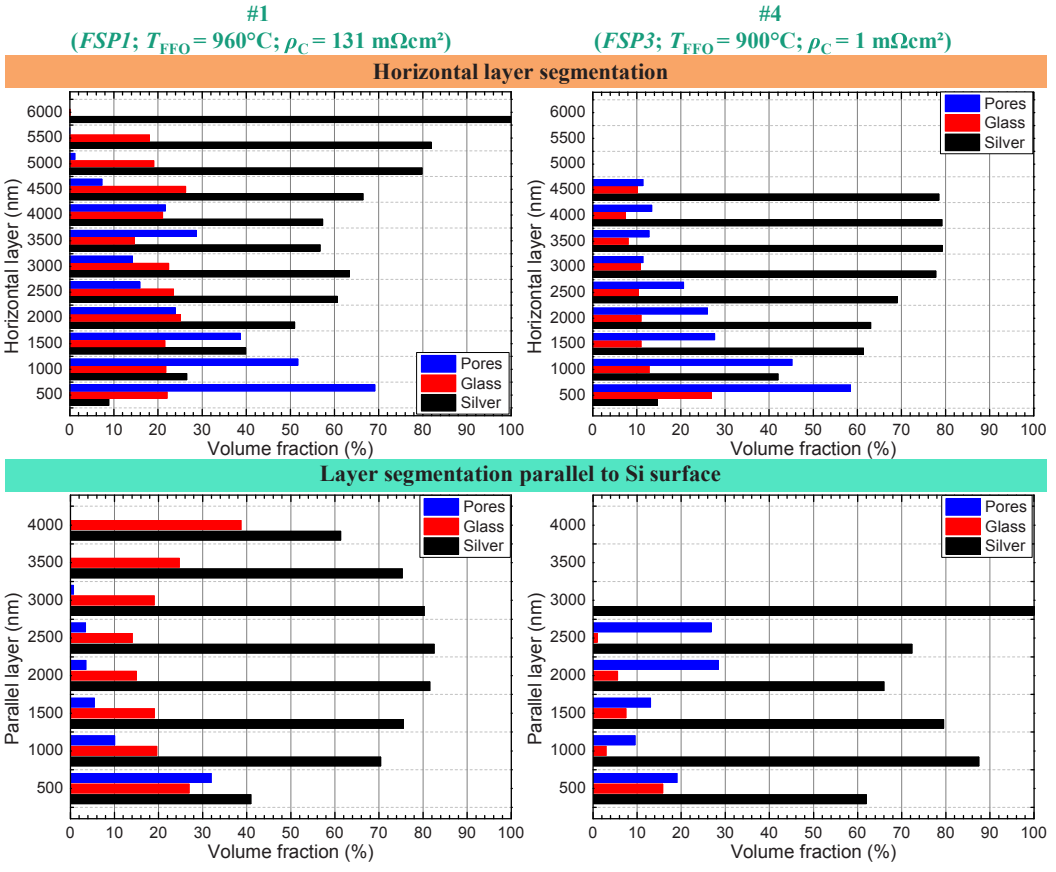

Fig. 3. Results of layer segmentation using focused ion beam tomography (FIB tomography) for two samples screen printed with different front side silver pastes *FSP* and fired at different set point peak firing temperatures T_{FFO}. FIB Tomogram sizes were 17.5 x 5.9 x 9.1 µm³ for sample #1 and 9.0 x 5.4 x 5.1 µm³ for sample #4. Electrical data of the sample can be found in Table 1, the principle of layer segmentation is displayed in Fig. 2. As obvious, a lower specific contact resistance (sample #4) correlates with a higher volume fraction of silver i) in the pyramid valleys of the alkaline textured Cz-Si (lower layers in horizontal segmentation) as well as ii) close to the emitter surface (lower layers in parallel segmentation).

As apparent from the horizontal layer segmentation, for both samples the volume fraction of silver increases significantly from bottom to top (pyramid valley to pyramid tip) whereas the volume fraction of glass and pores decreases. Especially the high volume fraction of pores is remarkable and important for modeling the electrical behavior of screen printed and fired silver contacts.

An accumulation of glass in the pyramid valleys as reported by Cabrera [6, 7] is also observed in this study. If the glass layer is assumed to be highly resistive, these microstructural properties would exclude a considerable contribution of the pyramid valleys to current transport. Furthermore, the lower contact resistance for sample #4 correlates with a lower amount of glass and pores in the lower and medium layers (horizontal segmentation) corresponding to pyramid valleys when compared to samples #1 and #2. The difference between these samples seems even more obvious for parallel layer segmentation: sample #4 reveals a significantly higher volume fraction of silver and therewith a lower fraction of pores and glass within the first 500 nm to 1000 nm. This layer is assumed to be significant for current transport due to its proximity to the emitter surface.

3.3. Investigating nano silver colloids in the glass layer

According to several authors, the glass layer between silicon emitter and front contact silver bulk is not necessarily electrically insulating, but can be essential for current conduction mechanisms [13-15, 19-21]. In particular Li and Cheng [13, 14] proposed a model of "nano-Ag colloid assisted tunnelling", where current paths through the glass layer along silver precipitates (in the nanometer range) are formed. In their studies, they also assumed that such a contact microstructure is more effective compared to contacts with numerous silver crystallites. Assuming the functionality of a silver enriched glass layer supporting current transport, we qualitatively and quantitatively investigated differently processed front side silver contacts by high resolution scanning electron microscopy (HR-SEM) and transmission electron microscopy (TEM).

Fig. 4 shows HR-SEM images of the samples #1, #2 and #3 with different measured specific contact resistances ρ_C. As it becomes clear from this figure, the amount of nano silver colloids present in the glass layer qualitatively correlates well with ρ_C. Sample #3, metallized with an improved silver paste *FSP2* providing significantly lower specific contact resistances after fast firing, shows also significantly more nano silver colloids, compared to the samples #1 (overfired) and #2 metallized with *FSP1*.

Nevertheless, statistical certainty still has to be proven for such quantitative evaluations and the inhomogeneity of screen printed silver contacts – especially on alkaline textured Cz-Si surfaces – has to be considered. However, classical current tunnelling models for metal-insulator-semiconductor structures mostly assume insulator layer thicknesses of only up to a few nanometers as well as applied forward voltages in the range of a few volts [11, 12]. Within this work HR-SEM (see Fig. 4) as well as TEM (see Fig. 5) investigations of the nano silver colloid containing glass phase always revealed colloid distances of several nanometers ($\geq$ 10 nm). Fig. 5 shows bright-field TEM (BF-TEM) images as well as an energy-filtered TEM (EFTEM) image of the glass layer for sample #1.

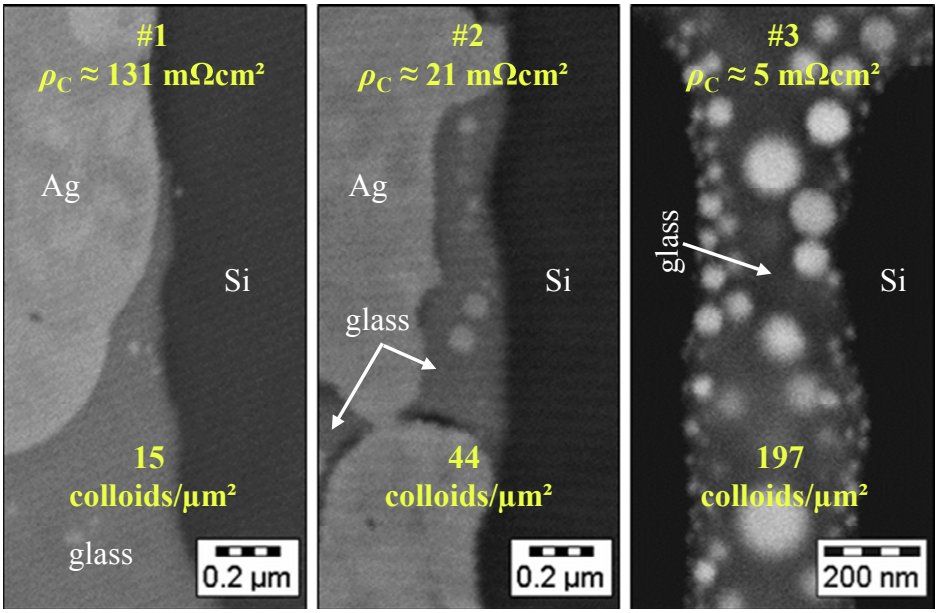

Fig. 4. Results of high resolution scanning electron microscopy imaging (HR-SEM) of the glass layer between silicon emitter and silver bulk for three differently processed front side silver contacts. Sample #3 metallized with the improved front side silver paste *FSP2* (providing lower specific contact resistances after fast firing) shows significantly more nano silver colloids in the glass layer. Current transport by nano silver colloid assisted tunneling [14] is conceivable but not self-evident. More data has to be acquired for statistically proven quantitative evaluations.

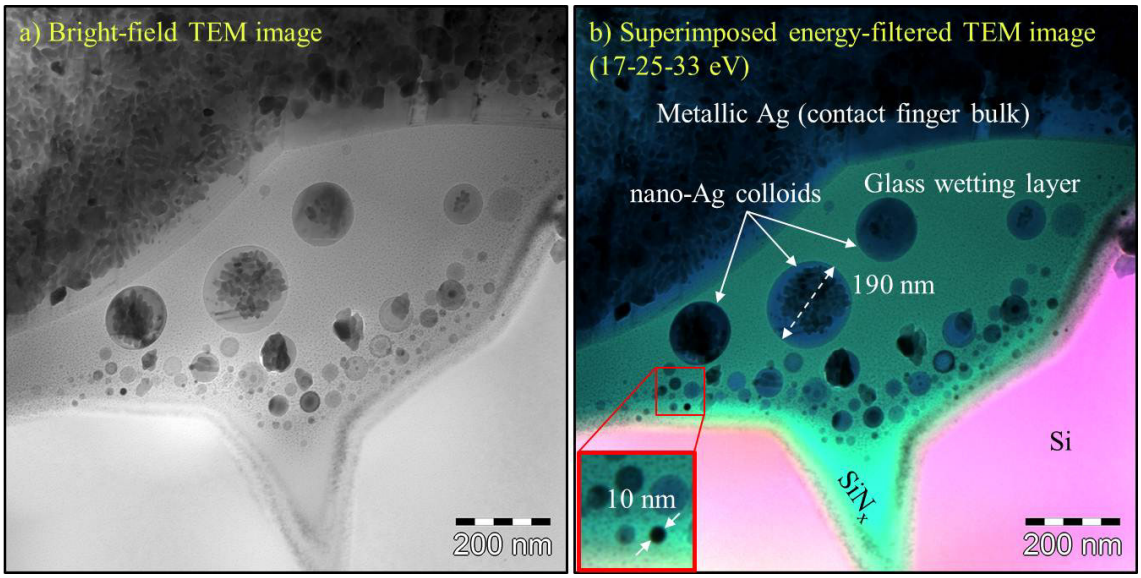

Fig. 5. a) Bright-field transmission electron microscopy (BF-TEM) image of the glass layer between silicon and silver bulk of the front side contact of sample #3 providing a low specific contact resistance b) Corresponding superimposed energy-filtered TEM (EFTEM) image, clearly indicating the different phases present at the silicon-silver contact interface: magenta = silicon, green = glass wetting layer (phase rich in SiO_2, containing also, among others, transition metals) black + blue = metallic silver. Elements and phases were additionally confirmed using energy-dispersive x-ray spectroscopy (EDX). Many nano silver colloids with diameters up to about 200 nm are detected, whereas colloids close to silicon tend to be smaller and colloids close to the silver bulk tend to be bigger. The colloids seem to appear in a kind of fine grain structure.

As these images show, many nano silver colloids can be found with diameters of up to about 200 nm. Colloids near the silicon interface tend to be smaller whereas colloids near the silver bulk of the contact finger tend to be bigger. The colloids seem to be microporous or mesoporous as can be seen by the fine grain structures of the colloids in Fig. 5 a). Diffraction contrast and Moiré fringe contrast yielded for the nano silver colloids indicate that they exist in crystalline phase. These images also clarify that no percolation paths are present and electrical current would always have to overcome glass layer distances in the range of ≥ 10 nm. In this case, (multi-step) tunnelling processes could not be explained with classical tunnelling theories such as direct tunnelling or Fowler-Nordheim tunnelling which assume (oxide) layer thicknesses in the range of just a few nanometers [11, 12]. For modelling current transport of screen printed and fired front side silver contacts by (multi-step) tunnelling processes, the glass layer should therefore not be assumed as an electrical insulator comparative to silicon oxide. Further investigations should focus on specifying the electrical properties of the glass layer in dependence on different process parameters applied.

4. Conclusion

Within the research project *MikroSol*, much effort was expended to itemize the microstructure of screen printed and fired front side silver contacts to explain contact formation and current transport mechanisms as well as electrical losses due to space charge region recombination induced by these contacts. Microstructural analyses of differently screen printed and fired front side contacts on alkaline textured surfaces were carried out using analytical electron microscopy and applying quantitative EDX spectroscopy in the SEM and TEM. In addition, 3D FIB tomography was applied on the same sample set. Microstructural data mostly correlated with the specific contact resistance measured by TLM.

It was found that screen printing silver pastes providing low specific contact resistances show a more pronounced wetting behavior of the silicon surface than pastes yielding higher specific contact resistances and thus lower solar cell efficiencies. Furthermore, a significantly higher density of nano silver colloids in the glass layer between the silicon surface and the silver bulk of the contact finger was found and studied by SEM and TEM techniques. Current transport through a thin glass layer by (multi-step) tunneling processes assisted by nano silver colloids is therefore conceivable (but not proven so far). TEM analysis revealed that these nano silver colloids exist in crystalline phase and measure up to 200 nm in diameter, whereas colloids near the silicon surface tend to be smaller and colloids close to the silver bulk of the contact finger tend to be larger. A continuous glass wetting layer for good contacting pastes was confirmed by FIB tomography. Additionally, extensive analysis of the 3D morphology of front side silver contacts by layer segmentation of FIB tomograms revealed a strong correlation between the volume fraction of the phases present in the metallization and the specific contact resistance of the contacts: low specific contact resistances correlate with a high volume fraction of silver (and less pores) within the first 500 nm to 1000 nm close to the emitter surface as well as in pyramid valleys (good coverage of silicon).

5. Acknowledgment

The Baden-Wuerttemberg Stiftung is gratefully acknowledged for financing these works within the research project "*MikroSol (U23)*". R. Hoenig acknowledges his supervisor Prof. Dr. Juergen Wilde for substantial support with fundamental knowledge in material sciences and characterization methods.

6. References

[1] R. Hoenig, *et al.*, "New measurement method for the investigation of space charge region recombination losses induced by the metallization of silicon solar cells," presented at the Proceedings of the 1st International Conference on Silicon Photovoltaics, Freiburg, Germany, 2011.

[2] R. Hoenig, *et al.*, "Impact of screen printing silver paste components on the space charge region recombination losses of industrial silicon solar cells " *Solar Energy Materials & Solar Cells* vol. 106, pp. 7-10, 2012.

[3] D. Pysch, *et al.*, "A review and comparison of different methods to determine the series resistance of solar cells," *Solar Energy Materials & Solar Cells,* vol. 91, pp. 1698-706, 2007.

[4] M. Glatthaar, *et al.*, "Spatially resolved determination of dark saturation current and series resistance of silicon solar cells," *Physica Status Solidi RRL,* vol. 4, pp. 13-15, 2010.

[5] G. K. Reeves and H. B. Harrison, "Obtaining the specific contact resistance from transmission line model measurements," *IEEE Electron Device Letters,* vol. EDL-3, pp. 111-3, 1982.

[6] E. Cabrera, *et al.*, "Experimental evidence of direct contact formation for the current transport in silver thick film metallized silicon emitters," *Journal of Applied Physics* vol. 110, pp. 114511-1-114511-5, 2011.

[7] E. Cabrera, *et al.*, "Influence of Surface Topography on the Glass Coverage in the Contact Formation of Silver Screen-Printed Si Solar Cells," *IEEE Journal of Photovoltaics,* vol. 3, pp. 102-107, 2013.

[8] C. Ballif, *et al.*, "Silver thick-film contacts on highly doped n-type silicon emitters: structural and electronic properties of the interface," *Applied Physics Letters,* vol. 82, pp. 1878-80, 2003.

[9] M. M. Hilali, *et al.*, " A review and understanding of screen-printed contacts and selective-emitter formation," in *Proceedings of the 14th Workshop on Crystalline Silicon Solar Cells and Modules NREL*, Winter Park, USA, 2004, pp. 109-16.

[10] G. Schubert, *et al.*, "Physical understanding of printed thick-film front contacts of crystalline Si solar cells—Review of existing models and recent developments," *Solar Energy Materials & Solar Cells,* vol. 90, pp. 3399-406, 2006.

[11] K. F. Schuegraf and C. Hu, "Hole Injection $Si0_2$ Breakdown Model for Very Low Voltage Lifetime Extrapolation," *IEEE Transactions On Electron Devices,* vol. 41, pp. 761-767, 1994.

[12] R. H. Fowler and L. Nordheim, "Electron Emission in Intense Electric Fields," *Proceedings of the Royal Society of London,* vol. Series A 119, pp. 173-181, 1928.

[13] L. K. Cheng, *et al.*, "Nano-Ag Colloids Assisted Tunneling Mechanism for Current Conduction in Front Contact of Crystalline Si Solar Cells," in *Proceedings of the 34th IEEE Photovoltaic Specialists Conference*, Philadelphia, USA, 2009.

[14] Z. G. L. Li, L. and Cheng, L.K., "Electron microscopy study of front-side Ag contact in crystalline Si solar cells," *Journal of Applied Physics,* vol. 105, p. 066102, 2009/03/18 2009.

[15] R. J. S. Young and A. F. Carroll, "Advances in front-side thick film metallisations for silicon solar cells," in *Proceedings of the 16th European Photovoltaic Solar Energy Conference*, Glasgow, UK, 2000, pp. 1731-4.

[16] M. Hörteis, "Fine-line printed contacts on crystalline silicon solar cells," Dissertation, Fachbereich Physik, Universität Konstanz, Konstanz, 2009.

[17] D. Pysch, *et al.*, "Comprehensive analysis of advanced solar cell contacts consisting of printed fine-line seed layers thickened by silver plating," *Progress in Photovoltaics: Research and Applications,* vol. 17, pp. 101-14, 2009.

[18] R. Hoenig, *et al.*, "Evaluation of Industrially Relevant Parameters for Contact Firing of Screen Printed Front Side Silver Contacts," in *Proceedings of the 3rd International Conference on Silicon Photovoltaics*, Hamelin, Germany, 2013.

[19] C.-H. Lin, *et al.*, "Investigation of Ag-bulk/glassy-phase/Si heterostructures of printed Ag contacts on crystalline Si solar cells," *Solar Energy Materials & Solar Cells,* vol. 92, pp. 1011-1015, 2008.

[20] T. Nakajima, *et al.*, "Ohmic contact of conductive silver paste to silicon solar cells " *The International journal for hybrid microelectronics,* vol. 6, pp. 580-8, 1983.

[21] M. Prudenziati, *et al.*, "Ag-based thick-film front metallization of silicon solar cells," *Active and passive electronic components,* vol. 13, pp. 133-50, 1989.